Alice Marmugi,[1] Julia Parnis,[1] Xi Chen,[2] LeAnne Carmichael,[1] Julie Hardy,[1] Naila Mannan,[1] Piero Marchetti,[3] Lorenzo Piemonti,[4] Domenico Bosco,[5] Paul Johnson,[6] James A.M. Shapiro,[7] Céline Cruciani-Guglielmacci,[8] Christophe Magnan,[8] Mark Ibberson,[9] Bernard Thorens,[10] Héctor H. Valdivia,[2] Guy A. Rutter,[1] and Isabelle Leclerc[1]

Sorcin Links Pancreatic β-Cell Lipotoxicity to ER Ca^{2+} Stores

Diabetes 2016;65:1009–1021 | DOI: 10.2337/db15-1334

Preserving β-cell function during the development of obesity and insulin resistance would limit the worldwide epidemic of type 2 diabetes. Endoplasmic reticulum (ER) calcium (Ca^{2+}) depletion induced by saturated free fatty acids and cytokines causes β-cell ER stress and apoptosis, but the molecular mechanisms behind these phenomena are still poorly understood. Here, we demonstrate that palmitate-induced sorcin downregulation and subsequent increases in glucose-6-phosphatase catalytic subunit-2 (G6PC2) levels contribute to lipotoxicity. Sorcin is a calcium sensor protein involved in maintaining ER Ca^{2+} by inhibiting ryanodine receptor activity and playing a role in terminating Ca^{2+}-induced Ca^{2+} release. *G6PC2*, a genome-wide association study gene associated with fasting blood glucose, is a negative regulator of glucose-stimulated insulin secretion (GSIS). High-fat feeding in mice and chronic exposure of human islets to palmitate decreases endogenous sorcin expression while levels of *G6PC2* mRNA increase. Sorcin-null mice are glucose intolerant, with markedly impaired GSIS and increased expression of *G6pc2*. Under high-fat diet, mice overexpressing sorcin in the β-cell display improved glucose tolerance, fasting blood glucose, and GSIS, whereas G6PC2 levels are decreased and cytosolic and ER Ca^{2+} are increased in transgenic islets. Sorcin may thus provide a target for intervention in type 2 diabetes.

Pancreatic β-cell dysfunction is central to the pathogenesis of type 2 diabetes. During the progression of obesity and insulin resistance, pancreatic islets of Langerhans initially increase β-cell mass and overproduce insulin (1). The increase in biosynthetic demand induced by chronic hyperglycemia activates the unfolded protein response (UPR), while increases in circulating free fatty acids and cytokines lower endoplasmic reticulum (ER) calcium (Ca^{2+}) stores (2,3), triggering ER stress and apoptosis if prolonged (4). The molecular mechanisms linking lipotoxicity and associated inflammation (5) to ER Ca^{2+} stores are largely unknown. Sorcin (gene name *SRI*) is a 22-kDa member of the penta-EF-hand family of calcium binding proteins that undergoes Ca^{2+}-dependent conformational changes (6–10). Sorcin is highly conserved among mammals and strongly expressed in primary mouse islets (11). In extrapancreatic cells, notably cardiac myocytes, sorcin associates with the ryanodine receptor (RyR) (12), the pore-forming α_1 subunit of voltage-dependent L-type Ca^{2+} channels (L-type VDCC) (13), and sarcoendoplasmic reticulum Ca^{2+} ATPase (SERCA) pumps (14) to modulate excitation-contraction coupling through changes in intracellular Ca^{2+} homeostasis (12). Sorcin inhibits RyR activity (15) and plays a role in terminating Ca^{2+}-induced Ca^{2+} release (12), an inherently self-sustaining mechanism that, if unchecked, may deplete intracellular Ca^{2+} stores (16).

We have recently shown that siRNA-mediated knockdown of sorcin in MIN6 insulinoma β-cells resulted in an apparent reduction in ER Ca^{2+} stores, as judged by stimulation with an inositol 1,4,5-triphosphate (IP3) mobilizing

[1]Section of Cell Biology and Functional Genomics, Division of Diabetes, Endocrinology & Metabolism, Department of Medicine, Imperial College London, London, U.K.
[2]Center for Arrhythmia Research, University of Michigan, Ann Arbor, MI
[3]Department of Endocrinology and Metabolism, University of Pisa, Pisa, Italy
[4]Diabetes Research Institute (HSR-DRI), San Raffaele Scientific Institute, Milan, Italy
[5]Cell Isolation and Transplantation Center, Department of Surgery, Geneva University Hospitals and University of Geneva, Geneva, Switzerland
[6]Nuffield Department of Surgical Sciences, University of Oxford, Oxford, U.K.
[7]Clinical Islet Laboratory and Clinical Islet Transplant Program, University of Alberta, Edmonton, Alberta, Canada
[8]Unit of Functional and Adaptive Biology, Paris Diderot University-Paris 7, Paris, France
[9]Vital-IT Group, SIB Swiss Institute of Bioinformatics, Lausanne, Switzerland
[10]Center for Integrative Genomics, University of Lausanne, Lausanne, Switzerland

Corresponding authors: Isabelle Leclerc, i.leclerc@imperial.ac.uk, and Guy A. Rutter, g.rutter@imperial.ac.uk.

Received 25 September 2015 and accepted 18 January 2016.

This article contains Supplementary Data online at http://diabetes.diabetesjournals.org/lookup/suppl/doi:10.2337/db15-1334/-/DC1.

agonist, and an inhibition of glucose-stimulated insulin secretion (GSIS) (17). These data indicated that sorcin may be required to maintain intracellular Ca^{2+} stores, possibly through its known capacity to inhibit RyRs (15) and activate SERCA pumps (14).

Since we and others have demonstrated that elevated palmitate (2) and cytokine levels (18,19) cause ER stress and apoptosis in pancreatic β-cells at least in part by decreasing ER Ca^{2+} stores (3), it follows that sorcin overexpression might protect against ER stress induced by inflammation and lipotoxicity. Indeed, recent data regarding human islets showed a decrease in sorcin expression induced by TNFα (20).

In the present report, we test this hypothesis using *1*) mice bearing null alleles of the sorcin gene ($Sri^{-/-}$), *2*) transgenic mouse lines overexpressing sorcin in the pancreatic β-cell, and *3*) adenovirus-mediated overexpression of sorcin in isolated human and murine islets.

RESEARCH DESIGN AND METHODS

Generation of Transgenic Mice Overexpressing Sorcin in Pancreatic β-Cells

Murine sorcin cDNA (17) was inserted in pBI-L vector (*Pvu*II-*Not*I sites), which contains a bidirectional Tet-responsive promoter driving the expression of both mSRI and firefly luciferase (21). After injection into the pronucleus of 0.5-day-old pure C57BL/6 fertilized oocytes (Embryonic Stem Cell and Transgenic Facility, Medical Research Council, London, U.K.), two founders, bearing 1 and 10 copies of the transgene (TetOn-*Sri*-1 and TetOn-*Sri*-10), were identified by PCR screening. β-Cell selectivity was achieved using the Tet-on system and RIP7-rtTA mice, which express the reverse tetracycline transactivator (rtTA) under the control of the rat insulin 2 promoter (21). Hemizygous TetOn-*Sri*-1 or -10 mice were crossed with homozygous RIP7-rtTA mice to generate double hemizygous TetOn-*Sri*/RIP7-rtTA (hereafter named SRI-tg1 and SRI-tg10) and single hemizygous RIP7-rtTA as littermate controls. Doxycycline (0.5 g/L in drinking water) and a high-fat diet (HFD; 60% kcal as fat, mainly saturated) were administered from 4 weeks of age unless specified otherwise.

Generation of Sorcin Knockout Mice

Homozygous sorcin-null mice ($Sri^{-/-}$) on a 129S1/SvImJ genetic background were generated by homologous recombination as previously described (22). In brief, the targeting construct was generated by flanking exon 3, present in both sorcin isoforms (accession no. NM_001080974.2 and NM_025618.3) with *loxP* sites for the Cre recombinase and inserting a phosphoglycerol kinase promoter–driven neomycin selection cassette flanked by an additional *loxP* site in the intron between exons 3 and 4.

Intraperitoneal Glucose and Insulin Tolerance Tests

Mice were fasted overnight for 14 h. Glucose solution (20% D-glucose/water, weight for volume, 1–3 g/kg body weight) or human regular insulin solution (0.5 or 1 units/kg, catalog no. 19278; Sigma-Aldrich) was administrated intraperitoneally and blood glucose was measured from the tail vein at 0, 15, 30, 60, 90, and 120 min using an ACCU-CHECK Aviva glucometer (Roche). Plasma insulin levels were measured using an ultrasensitive mouse insulin ELISA kit (Crystal Chem, Downers Grove, IL), and plasma glucose was assessed by Glucose Assay Kit (catalog no. 65333; Abcam) when above the glucometer detection limit.

Plasmids and Adenoviral Vectors

Plasmid pGL3-hG6PC2(−1075+124), containing the proximal promoter of the human glucose-6-phosphatase catalytic subunit-2 (*G6PC2*) gene upstream of luciferase reporter gene, was generated by PCR using human genomic DNA and the following primers: forward 5′-ACACG GTACCATCCTAGACACAATCCAGCTCTCT-3′ and reverse 5′-ACACAAGCTTTAAATGAAAAAGATATTCCTGGGG-3′. The resulting 1,220-bp fragment was subcloned into pCR2.1 by TA cloning, digested by *Kpn*I-*Xho*I, and subcloned into pGL3basic. A nuclear factor of activated T-cells (NFAT) luciferase reporter containing three tandem repeats of a 30-bp fragment of the IL-2 promoter for analysis of NFAT activity was a gift from Dr. Toren Finkel (Laboratory of Molecular Biology, National Heart, Lung, and Blood Institute, National Institutes of Health) (23). p5xATF6-GL3, containing five tandem repeats of ATF6 binding sites, was a gift from Ron Prywes (Department of Biological Sciences, Columbia University) (24). Plasmids pLKO.1-shSc (scrambled), pLKO.1-shSRI144, and pLKO.1-shSRI457 were constructed using the pLKO.1-TRC cloning vector from Addgene (plasmid no. 10878, protocol http://www.addgene.org/tools/protocols/plko/) and the oligonucleotides presented in Supplementary Table 1. Plasmid pAd-hSRI was generated by subcloning the human sorcin cDNA (pDNR-LIB-SRI) in pAdTrackCMV (*Bgl*III-*Hind*III sites). All the constructs were verified by DNA sequencing. The adenovirus Ad-hSRI-GFP was subsequently produced as in Noordeen et al. (17). Ad-mSRI-GFP encoding the murine sorcin cDNA and Ad-Null-GFP (empty vector) were described in Noordeen et al. (17).

Cell Culture, Transfection, and Luciferase Assays

MIN6 β-cells were used between passages 24 and 39 as in Noordeen et al. (17). Human and rat β-cell lines 1.1B4 and INS1(832/13) and HEK293 cells were cultured as in Noordeen et al. (25). Cells were transfected using Lipofectamine 2000 and Opti-Mem (Invitrogen), and luciferase assays were performed using a Dual-Luciferase Reporter Assay System (Promega) according to the manufacturer's instructions.

Human and Mouse Islets of Langerhans Isolation and Culture

Human islets from normoglycaemic donors were cultured as in Hodson et al. (26). Donor characteristics are presented in Supplementary Table 2. Pancreatic mouse islets were isolated and cultured as previously described (27). Transgenic islets were cultured in the presence of 0.5 μg/mL doxycycline to sustain transgene expression. Human and WT mouse islets (10-week-old C57BL/6 mice) were transduced with Ad-hSRI-GFP, Ad-mSRI-GFP, or

Ad-Null-GFP adenovirus at a multiplicity of infection of 100 for 48 h prior to total RNA extraction, GSIS, or intracellular Ca^{2+} imaging.

RNA Extraction, cDNA Synthesis, and Quantitative PCR Analysis

Total RNA was extracted, reversed transcribed, and analyzed as described in Sun et al. (28). Primers for SYBR Green assays are presented in Supplementary Table 3. Expression of each gene was normalized to β-actin and fold change in mRNA expression versus controls calculated using the $2^{-\Delta CT}$ method.

Microarray Analysis

Total RNA isolated from islets from 8-week-old, HFD-fed six SRI-tg10 male mice and six RIP7rtTA (littermate controls) was sent to the High Throughput Genomics Facility, Wellcome Trust Centre for Human Genetics, University of Oxford, and analyzed on Illumina MouseWG-6 v2 Expression BeadChips.

Ex Vivo Glucose–Stimulated Insulin Secretion

Insulin secretion assays on murine and human islets were performed as previously described in Leclerc et al. (29). Secreted and total insulin contents were quantified using a homogenous time-resolved fluorescence kit (HTRF) insulin kit (Cisbio).

Palmitate Treatment

Human islets were cultured for 72 h with either BSA or 0.5 mmol/L BSA-palmitate in 5.5 mmol/L glucose RPMI, and MIN6 cells were transduced with Ad-mSRI-GFP or Ad-Null-GFP adenoviruses for 24 h, prior to 48 h treatment with BSA or 0.5 mmol/L BSA-palmitate in 25 mmol/L glucose DMEM before total RNA extraction and qRT-PCR analysis.

Protein Extraction and Western Blotting

Western blotting was performed as in Leclerc et al. (29) using mouse monoclonal anti-sorcin (1:300, 25B3; Invitrogen) and mouse monoclonal anti–α-tubulin (1:10,000–20,000, catalog no. T5168; Sigma-Aldrich) antibodies.

Cytosolic Calcium Imaging

Imaging of free cytosolic Ca^{2+} concentration ($[Ca^{2+}]_{cyt}$) in isolated islets was performed using the trappable intracellular fluorescent Ca^{2+} dye Fura-2-AM (Invitrogen) (27). Imaging data were analyzed with ImageJ software using an in-house macro, and the fluorescence emission ratios were derived after subtracting background fluorescence.

ER Calcium Imaging

Clusters of isolated islets were transduced for 48 h with an adenovirus encoding the low-Ca^{2+}-affinity sensor D4 addressed to the ER, Ad-RIP-D4ER, as in Ravier et al. (30). Prior to acquisitions, cells were preincubated in Krebs-Ringer bicarbonate HEPES (KRBH) media (17) containing 3 mmol/L glucose for 1 h at 37°C and were perifused with KRBH supplemented with 17 mmol/L glucose and 250 μmol/L diazoxide (Diaz) (catalog no. D9035; Sigma-Aldrich) with the subsequent consecutive additions of 100 μmol/L acetyl-choline (catalog no. A2661; Sigma-Aldrich) and 1 μmol/L thapsigargin (catalog no. 586005; Calbiochem). Image analysis was performed as above.

Immunohistochemistry and Immunofluorescence Quantification of β– and α-Cell Mass

Analyses were performed as described in Sun et al. (28).

Statistical Analysis

Data are presented as means ± SEM. Significance was assessed by appropriate unpaired or paired two-tailed Student *t* tests or one- or two-way ANOVA as indicated, using GraphPad Prism 6.0 or Microsoft Excel. $P < 0.05$ was considered significant.

Study Approval

Studies involving human islets were approved by the National Research Ethics Committee London as detailed in Hodson et al. (26). All procedures involving animals received ethical approval and were compliant with the U.K. Animals (Scientific Procedures) Act 1986 or approved by the University Committee on Use and Care of Animals (University of Michigan, Ann Arbor, MI). Animals were housed two to five per individually ventilated cage in a pathogen-free facility with a 12-h light-dark cycle and had free access to food and water.

RESULTS

Sorcin Is Necessary for Normal Glucose Tolerance and Protects Against Lipotoxicity In Vivo

We previously reported that sorcin silencing in MIN6 cells leads to a complete abolition of ATP-evoked Ca^{2+} release from intracellular stores and an inhibition of GSIS (17). These findings prompted us to investigate the roles of sorcin in β-cell pathophysiology provoked by lipotoxicity, a condition known to trigger ER stress and β-cell failure (2).

In line with our findings in cell lines (17), sorcin-null mice ($Sri^{-/-}$, standard chow [SD] fed) displayed decreased glucose tolerance compared with sex-, weight-, and age-matched wild-type (WT) controls during intraperitoneal glucose tolerance tests (IPGTTs) (area under the curve [AUC], arbitrary units, WT vs. $Sri^{-/-}$, 2 months old: 43.5 ± 1.64 vs. 48.0 ± 1.1, n = 6–10, $P < 0.05$; 9 months old: 39.2 ± 2.5 vs. 49.1 ± 1.9, n = 4–7, $P < 0.01$) (Fig. 1*A* and *B*).

To determine whether sorcin overexpression might be protective against β-cell stress, we generated transgenic mice overexpressing sorcin in the pancreatic β-cell on the C57BL/6 genetic background, since males of this strain become glucose intolerant and insulin resistant under an HFD (31). Sorcin mRNA and protein levels were increased by at least twofold in isolated islets from SRI-tg1 and SRI-tg10 mice compared with those from littermate controls (Supplementary Fig. 1).

Glucose tolerance was improved in HFD-fed SRI-tg1 and SRI-tg10 male mice compared with their littermate controls during IPGTTs (AUC, arbitrary units, controls vs. SRI-tg1: 128.7 ± 6.1 vs. 101.2 ± 8.1, n = 7–8, $P < 0.05$; controls vs. SRI-tg10: 95.8 ± 5.4 vs. 73.0 ± 2.4, n = 9–13, $P < 0.001$) (Fig. 1*C* and *D*), despite similar insulin sensitivity as assessed by intraperitoneal insulin tolerance tests (IPITTs) (Fig. 1*E* and *F*, left panels) and body

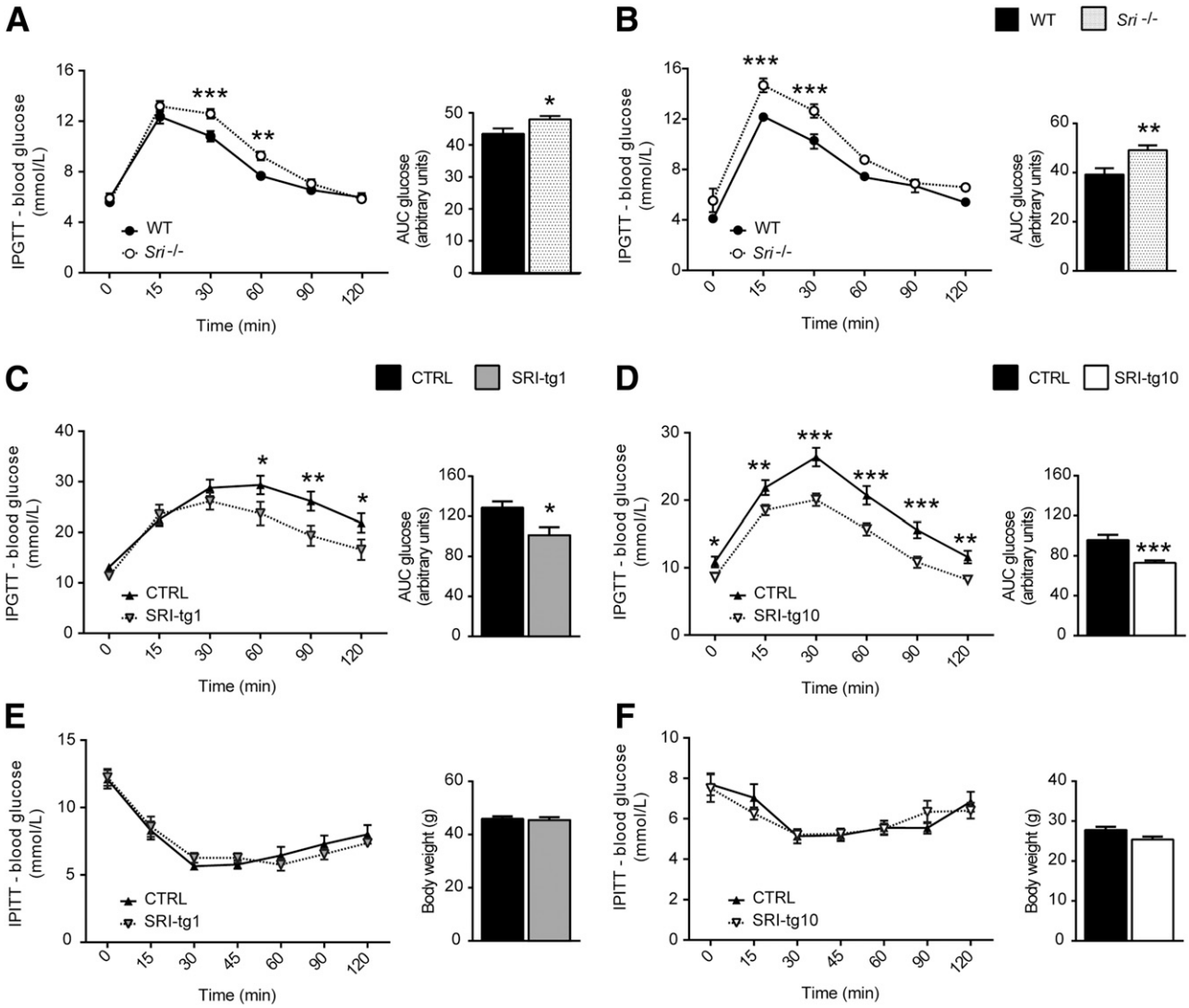

Figure 1—Sorcin deletion impairs glucose tolerance whereas sorcin overexpression in β-cells improves glucose tolerance during HFD. IPGTTs (1 g glucose/kg) were performed in SD-fed 2-month-old (*A*) and 9-month-old (*B*) $Sri^{-/-}$ male mice and sex-, weight-, and aged-matched WT controls (n = 4–10). IPGTTs (1 g glucose/kg) were performed in HFD-fed SRI-tg1 (n = 8–9, 16 weeks old) (*C*) and SRI-tg10 (n = 9–11, 8 weeks old) (*D*) male mice and littermate controls. Right panels represent AUC of blood glucose concentration during IPGTTs. IPITTs were performed in HFD-fed SRI-tg1 (n = 8–9, 17 weeks old, 1 unit insulin/kg) (*E*) and SRI-tg10 (n = 9–11, 9 weeks old, 0.5 units insulin/kg) (*F*) male mice and littermate controls. Right panels represent body weights for each group at the time of IPITTs. Values are means ± SEM. *$P < 0.05$; **$P < 0.01$; ***$P < 0.001$ (two-way ANOVA). CTRL, control.

weights (Fig. 1*E* and *F*, right panels). Remarkably, the above phenotype was not apparent in vivo in the absence of β-cell stress, i.e., during normal chow feeding (Supplementary Fig. 2).

Sorcin Enhances GSIS Without Increasing Pancreatic β-Cell Mass

We next investigated whether the changes in glucose tolerance observed in SRI-tg and $Sri^{-/-}$ mice were secondary to changes in insulin secretion. In vivo glucose-stimulated insulin release was assessed in SRI-tg10 and $Sri^{-/-}$ mice by IPGTTs (3 g glucose/kg body weight). As shown in Fig. 2*A* (top panel), plasma insulin concentrations were significantly higher at 30 min in SRI-tg10 compared with controls (plasma insulin, ng/mL, SRI-tg10 vs. controls, 30 min: 0.60 ± 0.06 vs. 0.43 ± 0.05, $P < 0.05$, n = 5–7), despite similar concomitant blood glucose values (Fig. 2*A*, bottom panel). Conversely, $Sri^{-/-}$ males showed a marked impairment of GSIS compared with WT controls, with plasma insulin concentrations barely rising during IPGTT (AUC insulin, WT vs. $Sri^{-/-}$, arbitrary units: 1.01 ± 0.23 vs. 0.53 ± 0.10, n = 4–6, $P < 0.05$) (Fig. 2*B*, top panel), despite robust increases in associated blood glucose values (Fig. 2*B* bottom panel).

We next explored whether the enhanced GSIS observed in SRI-tg10 islets might be secondary to an increase in β-cell mass. As shown in Fig. 2*C*–*E*, there were no significant changes in mean pancreas surface, islet size, individual β-cell or α-cell mass, although there was a significant decrease in β-cell to α-cell ratio.

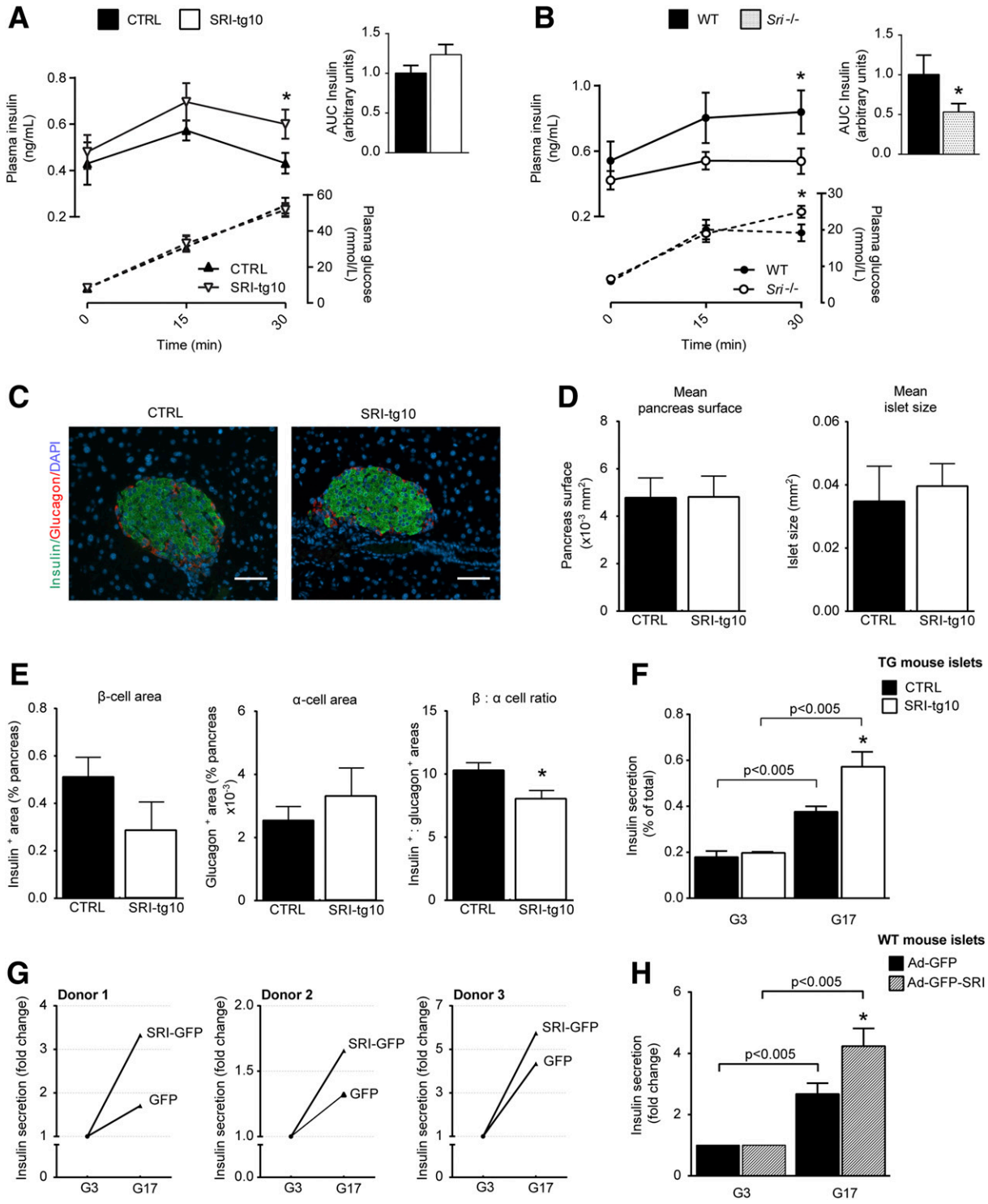

Figure 2—Sorcin overexpression enhances GSIS without expansion of β-cell mass, whereas sorcin deletion impairs GSIS. Plasma insulin concentration during 3 g glucose/kg IPGTTs were assessed in HFD-fed SRI-tg10 male mice (n = 5–7, 11 weeks old) (*A*) and SD-fed *Sri*$^{-/-}$ male mice (n = 4–6, 9 months old) (*B*) and their respective controls. Top left panels represent plasma insulin values and bottom panels represent corresponding blood glucose measurements. Top right panels represent AUC of plasma insulin concentrations. *C–F*: Pancreatic β-cell mass was evaluated in HFD-fed SRI-10 mice. Five consecutive pancreatic sections from 9-week-old SRI-tg10 and littermate control mice (n = 3–4) were immunostained for insulin, glucagon, and DAPI (scale bars = 50 μm) (*C*) to quantify for mean pancreas and islet size (*D*), and individual β-cell and α-cell area and β-cell to α-cell ratio as described in RESEARCH DESIGN AND METHODS (*E*). Ex vivo insulin secretion assays were performed in response to 3 or 17 mmol/L glucose (G3; G17) on isolated islets from HFD-fed transgenic (TG) SRI-tg10 male mice (n = 3, 27 weeks old) (*F*), human cadaveric donors (n = 3, see Supplementary Table 2 for donors characteristics) (*G*), and SD-fed WT C57BL/6 mice (n = 4–5, 10 weeks old) (*H*) transduced with an adenovirus encoding sorcin-GFP or GFP only as indicated. *P < 0.05 (in vivo GSIS/IPGTT: two-way ANOVA; β-cell mass and ex vivo GSIS: two-tailed Student t tests). CTRL, control.

The sorcin-induced improvement in in vivo GSIS was also observed ex vivo in islets isolated from SRI-tg1/10 mice and from human and mouse islets transduced for 48 h with an adenovirus encoding sorcin. Indeed, when stimulated with 17 mmol/L glucose, SRI-tg10 islets secreted 55% more insulin compared with control islets (insulin, percent of total, controls vs. SRI-tg10: 0.372 ± 0.02 vs. 0.577 ± 0.07, $n = 3$, $P < 0.05$), without any changes in insulin secretion at 3 mmol/L glucose (Fig. 2*F*), whereas SRI-tg1 islets secreted 68% more insulin at high glucose than controls (Supplementary Fig. 3). Adenovirus-mediated overexpression of sorcin consistently increased GSIS in human (Fig. 2*G*) and mouse (Fig. 2*H*) islets at 17 mmol/L glucose compared with islets transduced with a null-GFP virus.

Sorcin Improves Cytosolic Ca^{2+} Fluxes and Increases ER Ca^{2+} Stores

We next assessed whether the enhanced GSIS observed after sorcin overexpression was associated with changes in intracellular Ca^{2+} dynamics. Islets isolated from HFD-fed SRI-tg1 and SRI-tg10 mice were loaded with Fura-2 and perifused sequentially with low (3 mmol/L) and elevated (17 mmol/L) glucose concentrations. High glucose elicited a greater $[Ca^{2+}]_{cyt}$ response in sorcin-overexpressing islets compared with controls (AUC, arbitrary units, controls vs. SRI-tg1: 100.0 ± 5.0 vs. 120.1 ± 5.0, $n = 3$, $P < 0.05$ [Fig. 3*A*]; controls vs. SRI-tg10: 100.0 ± 17.80 vs. 149.9 ± 16.2, $n = 3$, $P < 0.05$ [Fig. 3*B*]). Likewise, transduction of dissociated human (Supplementary Fig. 4) or mouse (not shown) islets in vitro with sorcin-encoding adenoviruses significantly increased the number of islets displaying strong and high-amplitude $[Ca^{2+}]_{cyt}$ oscillations in response to 17 mmol/L glucose.

Free Ca^{2+} in the ER ($[Ca^{2+}]_{ER}$) was measured in clusters of isolated islets from HFD-fed SRI-tg1, SRI-tg10, and their littermate controls, transduced for 48 h with an adenovirus encoding the low-Ca^{2+}-affinity sensor D4 addressed to the

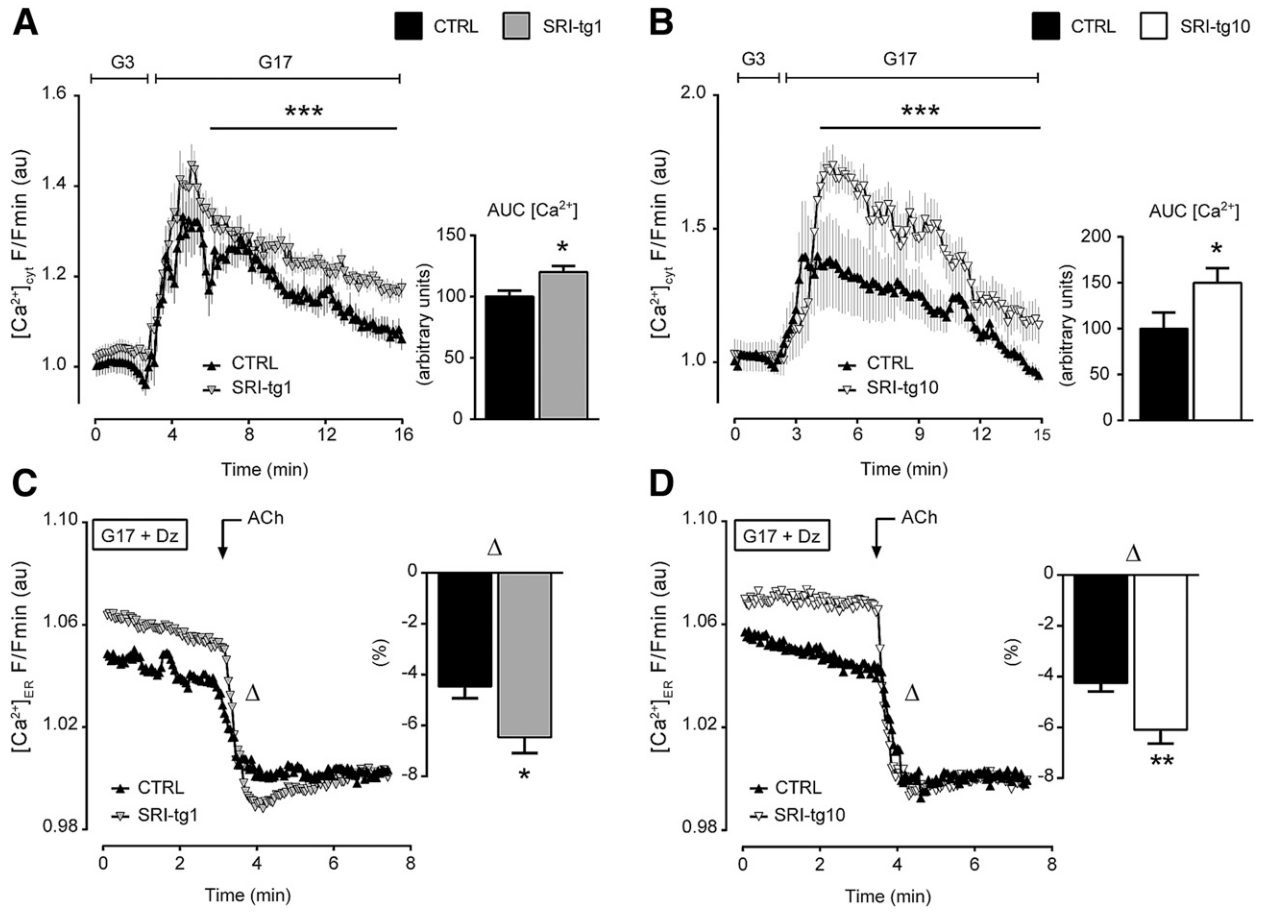

Figure 3—Sorcin overexpression increases intracellular Ca^{2+} fluxes and ER Ca^{2+} stores. Cytosolic Ca^{2+} levels ($[Ca^{2+}]_c$) were measured in isolated and dissociated islets loaded with Fura-2 from HFD-fed SRI-tg1 ($n = 3$–4, 14 weeks old) (*A*) and SRI-tg10 ($n = 3$, 9 weeks old) (*B*) male mice incubated sequentially with low (3 mmol/L, G3) and high (17 mmol/L, G17) glucose concentrations as indicated. Right panels represent AUC of $[Ca^{2+}]_c$. Acetylcholine (Ach)-induced ER Ca^{2+} release was measured in clusters of dissociated islets from HFD-fed SRI-tg1 ($n = 4$, 14 weeks old) (*C*) and SRI-tg10 ($n = 3$, 9 weeks old) (*D*) male mice transduced with Ad-RIP-D4ER adenovirus to measure $[Ca^{2+}]_{ER}$ as stated in RESEARCH DESIGN AND METHODS. The islets were incubated in 17 mmol/L glucose in the presence of Diaz (Dz; 250 μmol/L) to prevent extracellular Ca^{2+} influx. Left panels, representative calcium traces; right panels, quantification of the amplitude (Δ) of ER Ca^{2+} depletion after treatment with Ach. *$P < 0.05$; **$P < 0.01$; ***$P < 0.001$ ($[Ca^{2+}]_c$: two-way ANOVA; $[Ca^{2+}]_{ER}$ Δ: two-tailed Student *t* tests). au, arbitrary units; CTRL, control.

ER under the control of the insulin promoter Ad-RIP-D4ER (30), and incubated in 17 mmol/L glucose with the addition of 250 μmol/L Diaz to fully open ATP-sensitive K^+ channels and prevent extracellular Ca^{2+} influx (30). After acetylcholine-induced ER Ca^{2+} release, transgenic islets experienced a larger fall in $[Ca^{2+}]_{ER}$ than control islets, indicating a higher initial $[Ca^{2+}]_{ER}$ content (Fig. 3*C* and *D*). We next fully depleted the ER Ca^{2+} stores in islets isolated from HFD-fed SRI-tg10 male mice and littermate controls using the SERCA pump inhibitor cyclopiazonic acid (32,33) before measuring $[Ca^{2+}]_{cyt}$ in response to 17 mmol/L glucose. Under these conditions, the subsequent increase in $[Ca^{2+}]_{cyt}$ induced by high glucose was no longer significantly different between sorcin-overexpressing islets and control islets (AUC $[Ca^{2+}]_{cyt}$, arbitrary units, controls vs. SRI-tg10: 100.0 ± 13.5 vs. 104.6 ± 10.3, n = 3, NS) (Supplementary Fig. 5). Taken together, these results are consistent with a positive role for sorcin in GSIS and intracellular Ca^{2+} homeostasis, corroborating our in vitro data in MIN6 insulinoma cells (17).

Sorcin Regulates G6PC2 Expression Levels and Reduces Fasting Blood Glucose

To further explore the underlying mechanisms behind sorcin's actions, we performed a transcriptomic analysis of islets from HFD-fed SRI-tg10 mice and controls using oligonucleotide microarrays (GEO accession no. GSE72719) (Ingenuity Pathway Analysis presented in Supplementary Table 4). Interestingly, *G6pc2*, one of the most highly

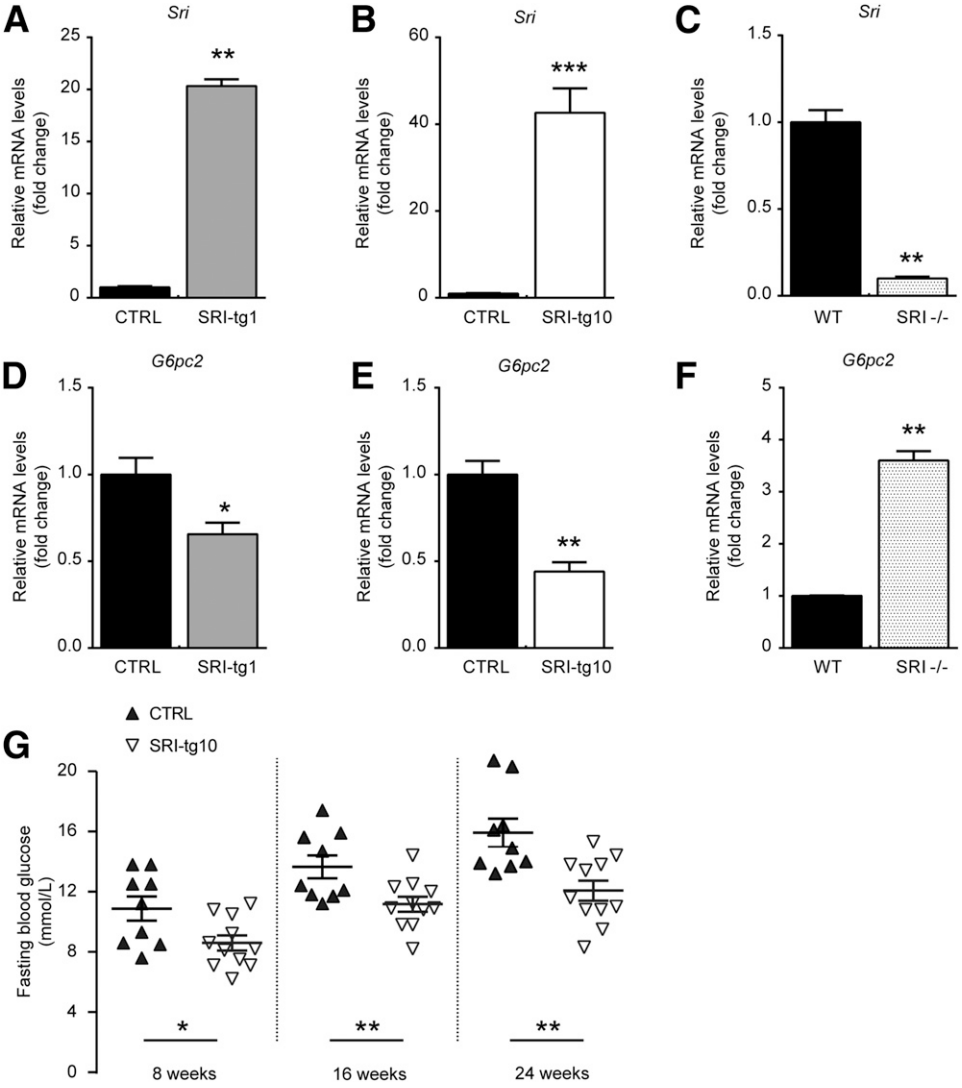

Figure 4—Sorcin regulates *G6pc2* expression and decreases fasting blood glucose in vivo. Quantitative RT-PCR analysis of *Sri* (*A–C*) and *G6pc2* (*D–F*) expression was performed in isolated islets from HFD-fed SRI-tg1 male (n = 3 mice/genotype, 27 weeks old) (*A* and *D*), SRI-tg10 male (n = 5 mice/genotype, 8 weeks old) (*B* and *E*), and SD-fed $SRI^{-/-}$ male (n = 4–7 mice/genotype, 9 months old) (*C* and *F*) mice and their respective controls. *G*: Fasting blood glucose levels were measured in HFD-fed SRI-tg10 male and their littermate control mice aged 8, 16, and 24 weeks, as indicated (n = 9–11 mice per group, HFD from 4 weeks old). *P < 0.05; **P < 0.01; ***P < 0.001 (two-tailed Student t tests). CTRL, control.

expressed genes in β-cells (9), was strongly repressed in islets from SRI-tg10 mice. Subsequent qRT-PCR analysis in isolated islets from SRI-tg10, SRI-tg1, and *Sri*$^{-/-}$ mice confirmed the inverse relationship between *Sri* and *G6pc2* expression levels (Fig. 4*A*–*F*). Indeed, islets from SRI-tg1 and SRI-tg10 mice displayed 35 and 56% decreases, respectively, in *G6pc2* mRNA levels (Fig. 4*D* and *E*), whereas *Sri* mRNA levels were increased 20- and 42-fold, respectively (Fig. 4*A* and *B*). In islets from *Sri*$^{-/-}$ mice, sorcin expression was reduced by >90% and there was a 3.6-fold increase in *G6pc2* expression (Fig. 4*C* and *F*). G6PC2 is an islet-specific isoform of glucose-6-phosphatase, which negatively regulates basal GSIS (9). G6PC2 is also a major determinant of fasting blood glucose in humans as revealed by genome-wide association studies (34). Accordingly, HFD-fed SRI-tg10 mice displayed lower fasting blood glucose throughout the study compared with controls (Fig. 4*G*).

Lipotoxic Conditions Decrease Endogenous Sorcin Expression in Mouse and Human Islets While Increasing G6PC2 and ER Stress Markers

We next overexpressed sorcin in human islets with an adenoviral vector and likewise observed a reduction in *G6PC2* mRNA levels, and in the levels of mRNA encoding the ER stress markers C/EBP homologous protein (*CHOP*) and glucose-regulated protein 78/binding immunoglobulin protein (*GRP78/BiP*) (Fig. 5*A*).

Given the apparent protection conferred by sorcin overexpression under lipotoxic conditions, we next investigated the regulation of endogenous sorcin during HFD in vivo and in human islets and MIN6 cells cultured in the presence of palmitate. Sorcin expression was downregulated in islets from HFD-fed C57BL/6 (Fig. 5*B*) and DBA2J mice (Supplementary Fig. 6) compared with chow-fed mice. Furthermore, human islets incubated for

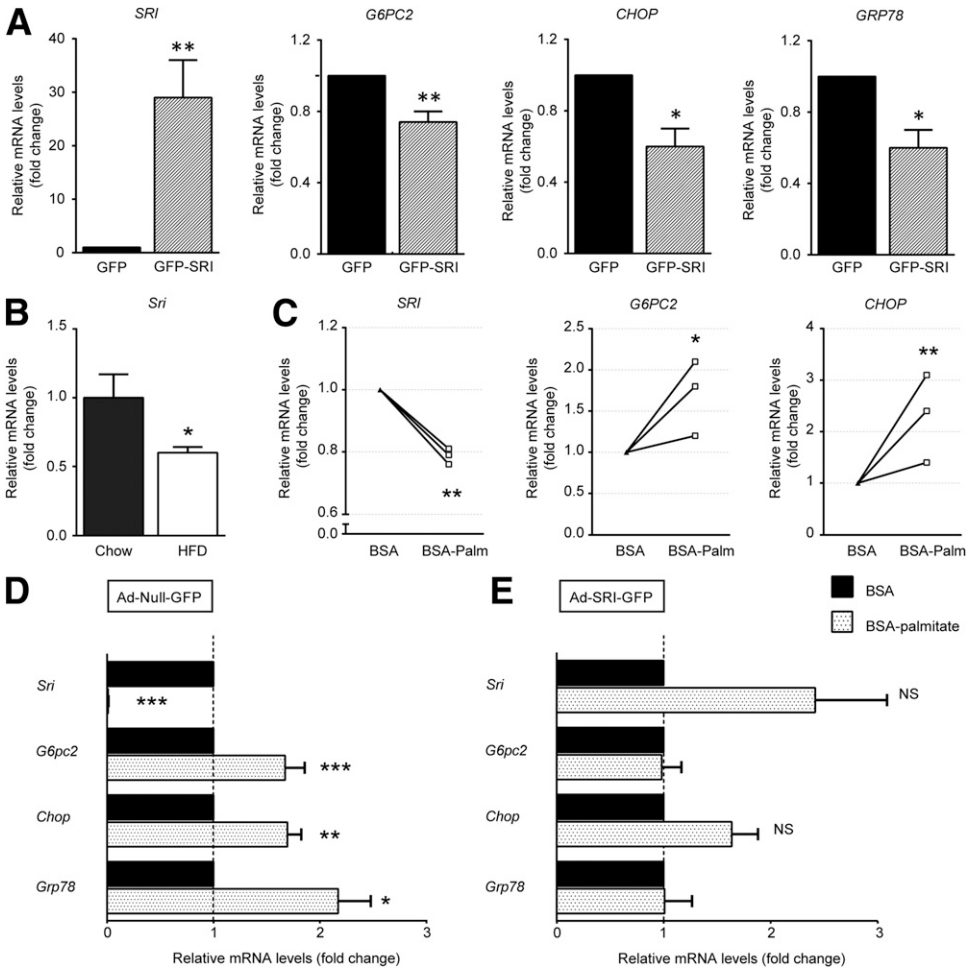

Figure 5—Lipotoxicity decreases endogeneous sorcin expression whereas sorcin overexpression prevents palmitate-induced G6PC2 and ER stress marker induction. *A*: Quantitative RT-PCR analysis of *SRI, G6PC2, CHOP*, and *GRP78/BiP* expression was performed on human islets (n = 3 donors) transduced for 48 h with either sorcin (GFP-SRI) or null (GFP) adenoviruses, as indicated. *B*: Quantitative RT-PCR analysis of *Sri* expression was performed in isolated islets from chow or HFD-fed WT mice (n = 4–5, 19-week-old females, HFD from 5 weeks old). Quantitative RT-PCR analysis of *SRI, G6PC2, CHOP*, and/or *GRP78/BiP* expression was performed on human islets (n = 3 donors) treated for 72 h with 0.5 mmol/L BSA-conjugated palmitate or BSA only (*C*) or on MIN6 β-cells transduced for 24 h with an adenovirus encoding GFP or sorcin-GFP followed by 48 h treatment with 0.5 mmol/L BSA-conjugated palmitate or BSA only (*D* and *E*). Values are mean ± SEM. *P < 0.05; **P < 0.01; ***P < 0.001 (two-tailed Student t tests).

72 h in the presence of palmitate and 5.5 mmol/L glucose showed a significant reduction in sorcin expression and an increase in *G6PC2* and *CHOP* expression (Fig. 5*C*). Similarly, lipotoxicity experiments in MIN6 cells also demonstrated a profound suppression of sorcin expression accompanied by a robust increase in *G6pc2*, *Chop*, and *Grp78/BiP* mRNA after exposure to palmitate (Fig. 5*D*). Remarkably, adenovirus-mediated overexpression of sorcin during lipotoxic conditions in MIN6 cells prevented the increase in *G6pc2*, *Chop*, and *Grp78/BiP* expression (Fig. 5*E*).

Sorcin Represses G6PC2 Promoter Activity Through NFAT Activation

We next determined whether the repressive effect of sorcin on G6PC2 expression was transcriptionally mediated. As shown in Fig. 6*A* (DMSO, gray bar), overexpressed sorcin repressed the activity of a 1.2-kb proximal fragment of the human *G6PC2* promoter (h*G6PC2*p) in MIN6 cells. Conversely, the activity of a reporter containing three tandem repeats of an NFAT binding site (3xNFATr) was significantly stimulated by sorcin (Fig. 6*B*, DMSO, gray bar), consistent with the increase in cytosolic $[Ca^{2+}]$ induced by sorcin (35). In order to confirm the roles of NFAT and $[Ca^{2+}]_{cyt}$ in mediating the inhibitory effect of sorcin on G6PC2 expression, we showed that NFAT cDNA cotransfection repressed h*G6PC2*p activity while robustly stimulating 3xNFATr (Fig. 6*A* and *B*, DMSO, black bars). In silico TRANSFAC analysis revealed three putative NFAT binding sites on *G6PC2* promoter (not shown). We next added Diaz (100 μmol/L, inhibiting Ca^{2+} influx) and cyclosporine A (CsA, 0.2 μmol/L, inhibiting NFAT nuclear translocation) in the culture medium. As expected, both agents prevented the inhibitory and stimulatory effects of sorcin on h*G6PC2*p and 3xNFATr, respectively (Fig. 6*A* and *B*, Diaz and CsA, gray bars). Moreover, the addition of CsA stimulated the activity of h*G6PC2*p compared with DMSO, whereas Diaz inhibited it (Supplementary Fig. 7), confirming the repressive contribution of the NFAT signaling pathway. The suppressive effect of Diaz, however, implies additional $[Ca^{2+}]_{cyt}$-dependent stimulatory pathways. Intriguingly, the addition of Diaz and CsA (up 1 μmol/L, not shown) did not prevent the inhibitory effects of NFAT on h*G6PC2*p but prevented the stimulatory effect of NFAT on 3xNFATr (Fig. 6*A* and *B*, Diaz and CsA, black bars).

Sorcin Activates ATF6 Transcriptional Activity

The inverse relationship between sorcin expression and the ER stress markers *CHOP* and *GRP78/BiP* prompted us to investigate the effect of sorcin on the UPR. To study the ATF6 branch (36), we chose a reporter assay containing five tandem repeats of ATF6 binding sites (24), since ATF6 is cleaved in the Golgi in response to ER stress before translocating to the nucleus (37). The activity of the ATF6 luciferase reporter was reproducibly stimulated by tunicamycin and thapsigargin, two ER stress inducers, and inhibited by the chemical chaperone 4-PBA, confirming its sensitivity to ER stress (Fig. 7*A–D*). Sorcin cotransfection increased the activity of the ATF6 luciferase reporter in three β-cell lines, i.e., MIN6, 1.1B4, and INS1 (832/13), as well as in HEK293 cells, in basal (DMSO) and stimulated (thapsigargin and tunicamycin) conditions, but not in the presence of 4-PBA, compared with cotransfection with GFP (Fig. 7*A–D*). Conversely, sorcin silencing in MIN6 cells by short hairpin RNA decreased the activity of the ATF6 reporter (Fig. 7*E* and *F*). Sorcin overexpression did not affect XBP-1 splicing, used as a surrogate of the IRE-1 branch, either in basal conditions or after thapsigargin treatment of MIN6 (Fig. 7G and *H*)

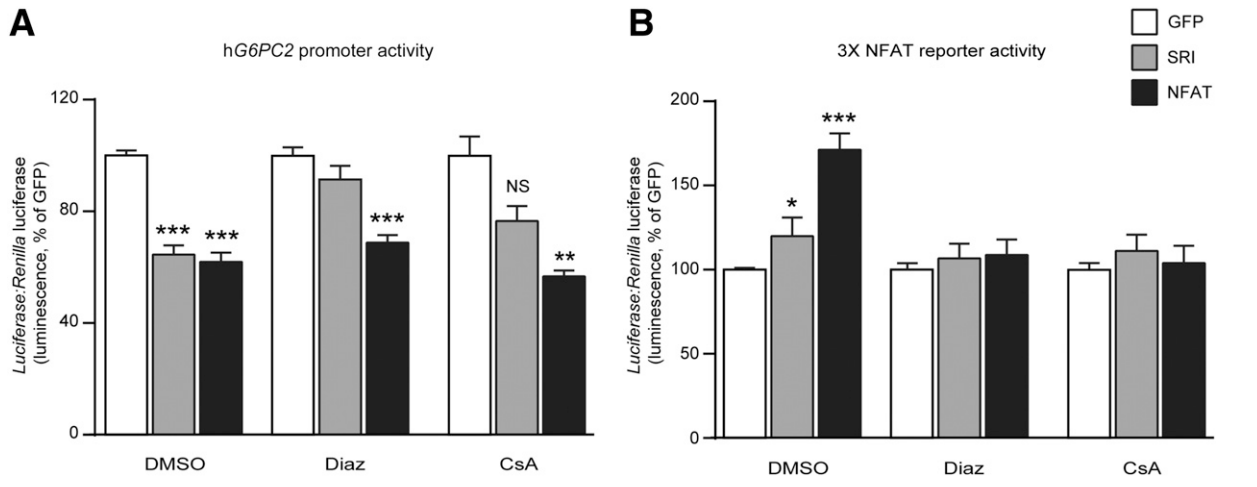

Figure 6— Sorcin inhibits G6PC2 promoter activity. Promoter luciferase reporter studies were performed in MIN6 β-cells cotransfected with either GFP (control), sorcin (SRI), or NFAT-GFP cDNAs and −1075+124hG6PC2-Luci (*A*) or three tandem repeats of NFAT binding sites (3× NFAT-Luci) and pRL-CMV (*B*) and treated with DMSO (0.1%), Diaz (100 μmol/L), or CsA (0.2 μmol/L) for an additional 24 h before cell lysis, as indicated (n = 3–4 independent experiments). Values are mean ± SEM. *P < 0.05; **P < 0.01; ***P < 0.001 (two-tailed Student t tests).

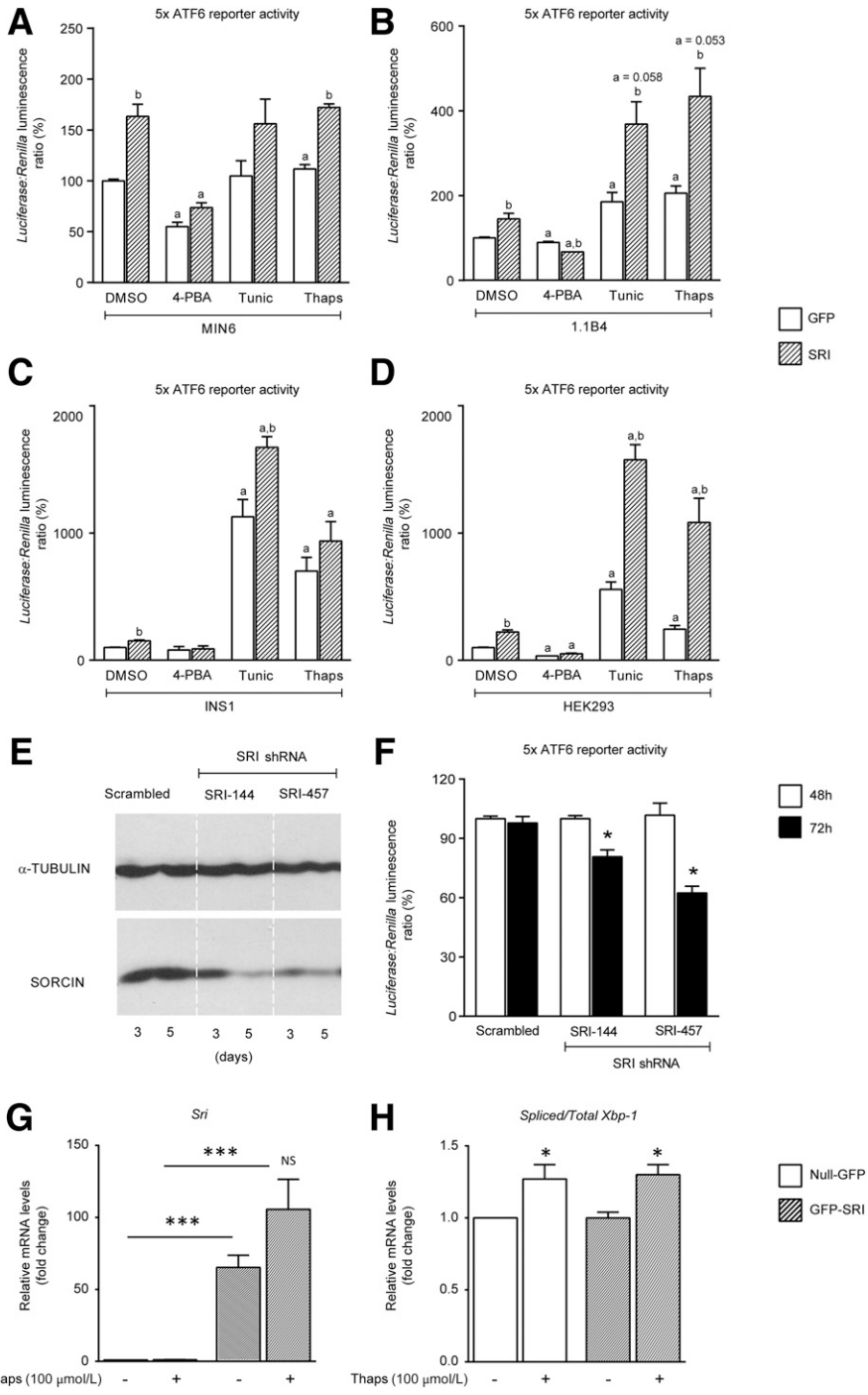

Figure 7—Sorcin (SRI) activates ATF6 transcriptional activity. Promoter luciferase reporter studies were performed in clonal β-cell lines MIN6 (*A*), 1.1B4 (*B*), INS1(832/13) (*C*), and human embryonic kidney HEK cells (*D*). Cells were cotransfected with an artificial promoter containing five ATF6 binding sites (p5xATF6-GL3), pRL-CMV, and either GFP or SRI cDNA for 24 h and treated with DMSO (1%), 4-PBA (10 mmol/L), tunicamycin (10 mg/mL), or thapsigargin (10 mmol/L) for an additional 16–20 h before cell lysis and luciferase assay. a, $P < 0.005$ for the effect of treatment vs. DMSO; b, $P < 0.05$ for the effect of SRI overexpression (unpaired two-tailed Student *t* tests). *E*: Western blot showing the efficiency of two different SRI short hairpin RNA constructs (shSRI-144 and shSRI-457) after 3 and 5 days in culture in MIN6 cells. Cells were transfected with either pLKO.1-shScrambled, -shSRI144, or -shSRI457 and incubated with 1 μg/mL puromycin for 3 or 5 days before cell lysis and Western blotting using polyclonal anti-SRI (1:300) and monoclonal anti-tubulin (1:10,000). Dashed vertical white lines have been added for clarity. *F*: SRI silencing reduces the activity of an artificial promoter containing five ATF6 binding sites in MIN6 cells. MIN6 were cotransfected with p5xATF6-GL3, pRL-CMV, and either pLKO.1-shScrambled, -shSRI144, or -shSRI457 for 48 or 72 h before cell lysis and luciferase assay. Results are expressed as mean ± SEM; $n = 3$ independent experiments. *$P < 0.005$, paired two-tailed Student *t* tests. Quantitative RT-PCR analysis of *Sri* (*G*) and spliced *Xbp1:total Xbp1* (*H*) was performed in MIN6 cells transduced for 24 h with adenoviruses encoding SRI-GFP or GFP only and treated with DMSO (0.1%) or thapsigargin (Thaps, 100 μmol/L) for an additional 24 h. Results are expressed as mean ± SEM; $n = 3$ independent experiments. *$P < 0.05$; ***$P < 0.005$ (paired two-tailed Student *t* tests).

or HEK293 (not shown) cells, whereas CHOP repression indicated repression of the PERK branch.

DISCUSSION

The findings herein indicate that sorcin lies on a pathway linking β-cell lipotoxicity to ER calcium and ER stress, representing a mechanism for dysregulation of β-cell function under conditions of metabolic stress (Fig. 8). Thus, we show that sorcin is downregulated in pancreatic β-cells under conditions of lipotoxic stress (Fig. 5), whereas overexpression of sorcin is sufficient to protect against β-cell failure and glucose intolerance during HFD (Fig. 1).

Interestingly, in the absence of β-cell stress, i.e., during normal chow feeding, the role of sorcin in pancreatic β-cells was less prominent. Nonetheless, forced sorcin expression enhanced GSIS and $[Ca^{2+}]_{cyt}$ oscillations in human islets from normoglycemic donors as well as in islets from young chow-fed mice (Fig. 2 and Supplementary Fig. 4). Importantly, the observed increase in GSIS in our transgenic models was not due to an increase in β-cell mass. Rather, we observed a decrease in the β-cell to α-cell ratio (Fig. 2), suggesting that the sorcin-overexpressing islets display enhanced function, and a possible resistance to HFD-induced hyperplasia (38). The improved GSIS observed in our HFD-fed SRI-tg1/10 mice is most likely secondary to the increases in glucose-induced intracellular Ca^{2+} fluxes (Fig. 3 and Supplementary Fig. 4). Although not tested here, the combined effects of RyR inhibition and SERCA activation by sorcin described in cardiomyocytes (14,15) might thus explain the increased capacity of ER Ca^{2+} stores in SRI-tg1/10 islets (Fig. 3). In the rat heart, sorcin overexpression is associated with an increase in Ca^{2+} transients and enhanced cardiac contractility, rescuing diabetic contractile dysfunction (39). In β-cells, a role for RyR, in particular RyR2, has recently been supported by studies using "leaky" mutants, both in humans and in mice, which display glucose intolerance, decreased insulin secretion, and islet ER stress (40,41).

One intriguing finding of the current study was the inverse relationship between sorcin and *G6PC2* expression in islets and β-cells. G6PC2 acts by hydrolyzing glucose-6-phosphate (G6P) in the ER, thus opposing the action of the glucokinase (9,42). Islets from *G6pc2*$^{-/-}$ mice display increased cytosolic $[Ca^{2+}]$ and enhanced GSIS (9). This suggests that an important mechanism of action of sorcin is to regulate *G6PC2* expression to influence calcium homeostasis, GSIS, and ER stress. Interestingly, others have found that glucose cycling and G6Pase activity were markedly enhanced in pancreatic islets of HFD-fed obese hyperglycemic mice, impairing GSIS (43). However, it is possible that G6PC2 also exerts effects beyond glucose cycling and glycolytic flux (44) and earlier studies have linked G6pase activity and G6P levels to cytosolic and ER Ca^{2+} concentrations, both in the liver and in pancreatic β-cells (45,46).

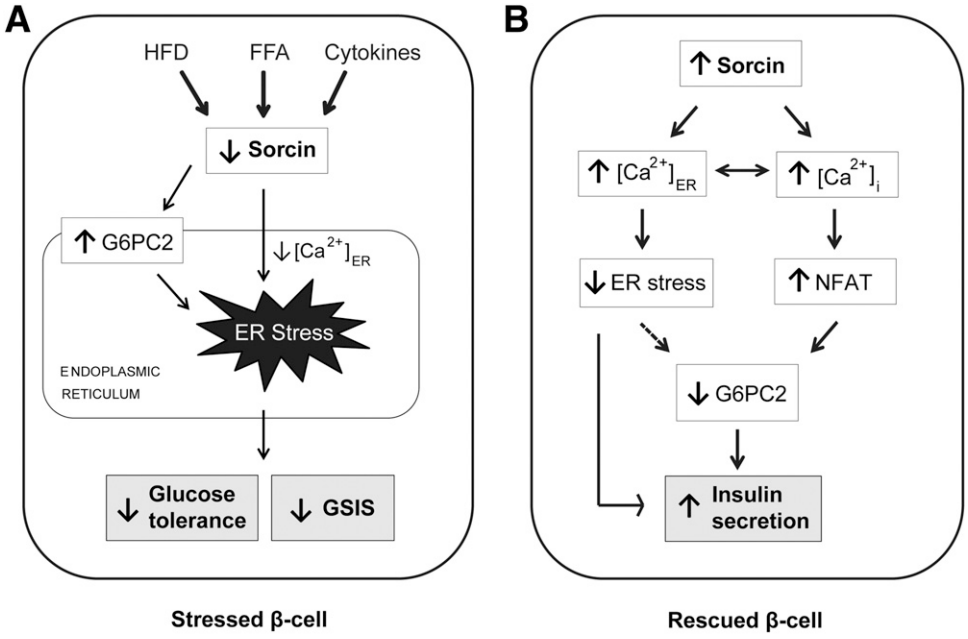

Figure 8—Sorcin lies on a pathway linking β-cell lipotoxicity to ER calcium and ER stress, representing a mechanism for dysregulation of β-cell function under conditions of metabolic stress. *A*: In pancreatic β-cells, sorcin is downregulated under conditions of lipotoxic stress such as exposure to HFD and palmitate or proinflammatory cytokines, as shown by others (20). The inverse relationship between sorcin and *G6PC2* expression levels observed in islets suggests that an important mechanism of action of sorcin is to regulate *G6PC2* expression to influence both ER stress and GSIS. *B*: Sorcin overexpression is sufficient to protect against β-cell dysfunction during HFD. In stressed β-cells, sorcin overexpression increases ER and cytosolic $[Ca^{2+}]$, decreasing G6PC2, through the NFAT signaling pathway, which would stimulate GSIS. By maintaining a high concentration of Ca^{2+} in the ER lumen, sorcin prevents ER stress and maintains long-term capacities for GSIS during HFD. FFA, free fatty acid.

Our study highlights several beneficial effects of sorcin in the β-cell. For example, sorcin-induced increase in intracellular Ca^{2+} activates NFAT signaling, which is fundamental for maintaining the islet β-cell phenotype (47), and whose inhibition is responsible for posttransplantation diabetes caused by calcineurin inhibitors (48). Furthermore, sorcin overexpression under lipotoxic conditions prevented the induction of the ER stress markers CHOP and GRP78/BiP. Interestingly, ATF6 signaling was stimulated by sorcin, a change that, unlike the other two branches of the UPR, i.e., PERK and IRE-1, is not usually associated with apoptosis but with favorable outcomes (36,49). We note that our data may also have direct relevance for β-cell failure in humans. Thus, analysis of unpublished results from the IMIDIA consortium (M. Solimena, A.M. Schulte, L. Marselli, F. Ehehalt, D. Richter, M. Rösler, H. Mziaut, K.-P. Knoch, J.P., M. Bugliani, A. Siddiq, A. Jörns, F. Burdet, R. Liechti, M. Suleiman, D. Margerie, F. Syed, M. Distler, R. Grützmann, E. Petretto, A. Moreno, C. Wegbrod, A. Sönmez, K. Pfriem, A. Friedrich, J. Meinel, C. Wollheim, G. Baretton, R. Scharfmann, E. Nogoceke, E. Bonifacio, D. Sturm, U. Boggi, H.-D. Saeger, F. Filipponi, M. Lesche, P. Meda, A. Dahl, L. Wigger, I. Xenarios, M. Falchi, B.T., J. Weitz, K. Bokvist, S. Lenzen, G.A.R., P. Froguel, M. von Bülow, M.I., P.M., unpublished data) from large sets of human donor islets indicates a significant positive correlation between *SRI* mRNA levels and GSIS in both diabetic and nondiabetic islets, and a tendency toward lower sorcin levels in islets from patients with type 2 diabetes versus healthy islets. Thus, agents that increase sorcin expression or activity may increase insulin secretion while protecting against β-cell exhaustion.

Acknowledgments. The authors thank Anke Schulte (Sanofi Aventis, Frankfurt, Germany) and Michel Solimena (Technical University, Dresden, Germany) for sharing expression data on sorcin in human islets ahead of publication. The authors thank Pauline Chabosseau (Imperial College London) for help in designing macros for Ca^{2+} imaging and β-cell mass measurements. The authors thank the High-Throughput Genomics Group at the Wellcome Trust Centre for Human Genetics (University of Oxford) for the generation of the gene expression data.

Funding. This study was supported by the European Foundation for the Study of Diabetes (Albert Renold Travel Fellowship/94386 to A.M.), the National Institutes of Health (grants R01-HL120108 and R01-HL055438 to H.H.V.), and Diabetes UK (BDA:12/0004535 to I.L.). G.A.R. was supported by grants from the Wellcome Trust (WT098424AIA), the Medical Research Council (Programme MR/J0003042/1), and the Biotechnology and Biological Sciences Research Council (BB/J015873/1). The work leading to this publication also received support from the Innovative Medicines Initiative Joint Undertaking under grant agreement no. 155005 (IMIDIA) (P.M., C.M., B.T., and G.A.R.), resources of which are composed of a financial contribution from the European Union's Seventh Framework Programme (FP7/2007-2013) and European Federation of Pharmaceutical Industries and Associations companies' in-kind contribution. G.A.R. is a Royal Society Wolfson Research Merit Award holder.

Duality of Interest. No potential conflicts of interest relevant to this article were reported.

Author Contributions. A.M. designed research studies, conducted experiments, acquired and analyzed data, and wrote the manuscript. J.P. conducted experiments and acquired and analyzed data. X.C., J.H., and N.M. conducted experiments and acquired data. L.C. conducted experiments, acquired data, and wrote the manuscript. P.M., L.P., D.B., P.J., and J.A.M.S. provided human islets. C.C.-G., C.M., and B.T. provided IMIDIA data. M.I. performed a bioinformatics analysis of IMIDIA data. H.H.V. provided $Sri^{-/-}$ mice and polyclonal anti-SRI antibody. G.A.R. designed research studies, analyzed data, provided reagents, and wrote the manuscript. I.L. designed research studies, conducted experiments, acquired and analyzed data, provided reagents, and wrote the manuscript. I.L. is the guarantor of this work and, as such, had full access to all the data in the study and takes responsibility for the integrity of the data and the accuracy of the data analysis.

Prior Presentation. This study was presented at the 2014 Diabetes UK Professional Conference, 5–7 March 2014, Liverpool, U.K.; the 2015 Diabetes UK Professional Conference, 11–13 March 2015, London, U.K.; the 50th Annual Meeting of the European Association for the Study of Diabetes (EASD), 15–19 September 2014, Vienna, Austria; the 51st Annual Meeting of the EASD, 14–18 September 2015, Stockholm, Sweden; and the 31st Congress of the French Society of Endocrinology, 5–8 November 2014, Lyon, France.

References

1. Prentki M, Nolan CJ. Islet beta cell failure in type 2 diabetes. J Clin Invest 2006;116:1802–1812
2. Cunha DA, Hekerman P, Ladrière L, et al. Initiation and execution of lipotoxic ER stress in pancreatic beta-cells. J Cell Sci 2008;121:2308–2318
3. Ramadan JW, Steiner SR, O'Neill CM, Nunemaker CS. The central role of calcium in the effects of cytokines on beta-cell function: implications for type 1 and type 2 diabetes. Cell Calcium 2011;50:481–490
4. Arruda AP, Hotamisligil GS. Calcium homeostasis and organelle function in the pathogenesis of obesity and diabetes. Cell Metab 2015;22:381–397
5. Hotamisligil GS. Endoplasmic reticulum stress and the inflammatory basis of metabolic disease. Cell 2010;140:900–917
6. Ilari A, Johnson KA, Nastopoulos V, et al. The crystal structure of the sorcin calcium binding domain provides a model of Ca2+-dependent processes in the full-length protein. J Mol Biol 2002;317:447–458
7. Van der Bliek AM, Meyers MB, Biedler JL, Hes E, Borst P. A 22-kd protein (sorcin/V19) encoded by an amplified gene in multidrug-resistant cells, is homologous to the calcium-binding light chain of calpain. EMBO J 1986;5:3201–3208
8. Valdivia HH. Modulation of intracellular Ca2+ levels in the heart by sorcin and FKBP12, two accessory proteins of ryanodine receptors. Trends Pharmacol Sci 1998;19:479–482
9. Pound LD, Oeser JK, O'Brien TP, et al. G6PC2: a negative regulator of basal glucose-stimulated insulin secretion. Diabetes 2013;62:1547–1556
10. Meyers MB, Biedler JL. Increased synthesis of a low molecular weight protein in vincristine-resistant cells. Biochem Biophys Res Commun 1981;99:228–235
11. Kone M, Pullen TJ, Sun G, et al. LKB1 and AMPK differentially regulate pancreatic β-cell identity. FASEB J 2014;28:4972–4985
12. Farrell EF, Antaramian A, Rueda A, Gómez AM, Valdivia HH. Sorcin inhibits calcium release and modulates excitation-contraction coupling in the heart. J Biol Chem 2003;278:34660–34666
13. Meyers MB, Puri TS, Chien AJ, et al. Sorcin associates with the pore-forming subunit of voltage-dependent L-type Ca2+ channels. J Biol Chem 1998;273:18930–18935
14. Matsumoto T, Hisamatsu Y, Ohkusa T, et al. Sorcin interacts with sarcoplasmic reticulum Ca(2+)-ATPase and modulates excitation-contraction coupling in the heart. Basic Res Cardiol 2005;100:250–262
15. Lokuta AJ, Meyers MB, Sander PR, Fishman GI, Valdivia HH. Modulation of cardiac ryanodine receptors by sorcin. J Biol Chem 1997;272:25333–25338
16. Stern MD, Cheng H. Putting out the fire: what terminates calcium-induced calcium release in cardiac muscle? Cell Calcium 2004;35:591–601
17. Noordeen NA, Meur G, Rutter GA, Leclerc I. Glucose-induced nuclear shuttling of ChREBP is mediated by sorcin and Ca(2+) ions in pancreatic β-cells. Diabetes 2012;61:574–585

18. Riboulet-Chavey A, Diraison F, Siew LK, Wong FS, Rutter GA. Inhibition of AMP-activated protein kinase protects pancreatic beta-cells from cytokine-mediated apoptosis and CD8+ T-cell-induced cytotoxicity. Diabetes 2008;57:415–423
19. Cardozo AK, Ortis F, Storling J, et al. Cytokines downregulate the sarcoendoplasmic reticulum pump Ca2+ ATPase 2b and deplete endoplasmic reticulum Ca2+, leading to induction of endoplasmic reticulum stress in pancreatic beta-cells. Diabetes 2005;54:452–461
20. Rutti S, Arous C, Schvartz D, et al. Fractalkine (CX3CL1), a new factor protecting β-cells against TNFα. Mol Metab 2014;3:731–741
21. Pullen TJ, Sylow L, Sun G, Halestrap AP, Richter EA, Rutter GA. Overexpression of monocarboxylate transporter-1 (SLC16A1) in mouse pancreatic β-cells leads to relative hyperinsulinism during exercise. Diabetes 2012;61:1719–1725
22. Chen X, Valdivia CR, Weber C, Powers PA, Valdivia HH. Abstract 13891: enhanced sodium-calcium exchanger current, prolonged action potential duration, and early/delayed-afterdepolarization in sorcin knockout heart. Circulation 2014;130:A13891
23. Ichida M, Finkel T. Ras regulates NFAT3 activity in cardiac myocytes. J Biol Chem 2001;276:3524–3530
24. Wang Y, Shen J, Arenzana N, Tirasophon W, Kaufman RJ, Prywes R. Activation of ATF6 and an ATF6 DNA binding site by the endoplasmic reticulum stress response. J Biol Chem 2000;275:27013–27020
25. Noordeen NA, Khera TK, Sun G, et al. Carbohydrate-responsive element-binding protein (ChREBP) is a negative regulator of ARNT/HIF-1beta gene expression in pancreatic islet beta-cells. Diabetes 2010;59:153–160
26. Hodson DJ, Mitchell RK, Bellomo EA, et al. Lipotoxicity disrupts incretin-regulated human β cell connectivity. J Clin Invest 2013;123:4182–4194
27. Ravier MA, Rutter GA. Isolation and culture of mouse pancreatic islets for ex vivo imaging studies with trappable or recombinant fluorescent probes. Methods Mol Biol 2010;633:171–184
28. Sun G, Tarasov AI, McGinty JA, et al. LKB1 deletion with the RIP2. Cre transgene modifies pancreatic beta-cell morphology and enhances insulin secretion in vivo. Am J Physiol Endocrinol Metab 2010;298:E1261–E1273
29. Leclerc I, Woltersdorf WW, da Silva Xavier G, et al. Metformin, but not leptin, regulates AMP-activated protein kinase in pancreatic islets: impact on glucose-stimulated insulin secretion. Am J Physiol Endocrinol Metab 2004;286:E1023–E1031
30. Ravier MA, Daro D, Roma LP, et al. Mechanisms of control of the free Ca2+ concentration in the endoplasmic reticulum of mouse pancreatic β-cells: interplay with cell metabolism and [Ca2+]c and role of SERCA2b and SERCA3. Diabetes 2011;60:2533–2545
31. Surwit RS, Feinglos MN, Rodin J, et al. Differential effects of fat and sucrose on the development of obesity and diabetes in C57BL/6J and A/J mice. Metabolism 1995;44:645–651
32. Ainscow EK, Rutter GA. Glucose-stimulated oscillations in free cytosolic ATP concentration imaged in single islet beta-cells: evidence for a Ca2+-dependent mechanism. Diabetes 2002;51(Suppl. 1):S162–S170
33. Mitchell KJ, Pinton P, Varadi A, et al. Dense core secretory vesicles revealed as a dynamic Ca(2+) store in neuroendocrine cells with a vesicle-associated membrane protein aequorin chimaera. J Cell Biol 2001;155:41–51
34. Bouatia-Naji N, Rocheleau G, Van Lommel L, et al. A polymorphism within the G6PC2 gene is associated with fasting plasma glucose levels. Science 2008; 320:1085–1088
35. Crabtree GR, Olson EN. NFAT signaling: choreographing the social lives of cells. Cell 2002;109(Suppl.):S67–S79
36. Szegezdi E, Logue SE, Gorman AM, Samali A. Mediators of endoplasmic reticulum stress-induced apoptosis. EMBO Rep 2006;7:880–885
37. Ye J, Rawson RB, Komuro R, et al. ER stress induces cleavage of membrane-bound ATF6 by the same proteases that process SREBPs. Mol Cell 2000;6:1355–1364
38. Gao M, Ma Y, Liu D. High-fat diet-induced adiposity, adipose inflammation, hepatic steatosis and hyperinsulinemia in outbred CD-1 mice. PLoS One 2015; 10:e0119784
39. Suarez J, Belke DD, Gloss B, et al. In vivo adenoviral transfer of sorcin reverses cardiac contractile abnormalities of diabetic cardiomyopathy. Am J Physiol Heart Circ Physiol 2004;286:H68–H75
40. Santulli G, Pagano G, Sardu C, et al. Calcium release channel RyR2 regulates insulin release and glucose homeostasis. J Clin Invest 2015;125:1968–1978
41. Dixit SS, Wang T, Manzano EJ, et al. Effects of CaMKII-mediated phosphorylation of ryanodine receptor type 2 on islet calcium handling, insulin secretion, and glucose tolerance. PLoS One 2013;8:e58655
42. Wall ML, Pound LD, Trenary I, O'Brien RM, Young JD. Novel stable isotope analyses demonstrate significant rates of glucose cycling in mouse pancreatic islets. Diabetes 2015;64:2129–2137
43. Ling ZC, Khan A, Delauny F, et al. Increased glucocorticoid sensitivity in islet beta-cells: effects on glucose 6-phosphatase, glucose cycling and insulin release. Diabetologia 1998;41:634–639
44. Marcolongo P, Fulceri R, Gamberucci A, Czegle I, Banhegyi G, Benedetti A. Multiple roles of glucose-6-phosphatases in pathophysiology: state of the art and future trends. Biochim Biophys Acta 2013;1830:2608–2618
45. Wolf BA, Colca JR, Comens PG, Turk J, McDaniel ML. Glucose 6-phosphate regulates Ca2+ steady state in endoplasmic reticulum of islets. A possible link in glucose-induced insulin secretion. J Biol Chem 1986;261:16284–16287
46. Benedetti A, Fulceri R, Comporti M. Calcium sequestration activity in rat liver microsomes. Evidence for a cooperation of calcium transport with glucose-6-phosphatase. Biochim Biophys Acta 1985;816:267–277
47. Heit JJ, Apelqvist AA, Gu X, et al. Calcineurin/NFAT signalling regulates pancreatic beta-cell growth and function. Nature 2006;443:345–349
48. Weir MR, Fink JC. Risk for posttransplant diabetes mellitus with current immunosuppressive medications. Am J Kidney Dis 1999;34:1–13
49. Sharma RB, O'Donnell AC, Stamateris RE, et al. Insulin demand regulates β cell number via the unfolded protein response. J Clin Invest 2015;125:3831–3846